HEDLA 2010: Hydrodynamics of Hypersonic Jets: Experiments and Numerical Simulations

Marco Belan, Sergio de Ponte, **Daniela Tordella**,
Silvano Massaglia, Attilio Ferrari, Andrea Mignone,
Eberhard Bodenschatz

ALMA UNIVERSITAS TAURINENSIS

MAX-PLANCK-GESELLSCHAFT

1 Aim

To understand whether,
without the intervention of magnetic fields,

hypersonic Newtonian jets produce any similarity to the morphologies observed in astrophysical jets,

we have conceived a laboratory experiment and performed three-dimensional numerical simulations which reproduce the mid-long term evolution of hypersonic jets.

2 The experiment: facilities

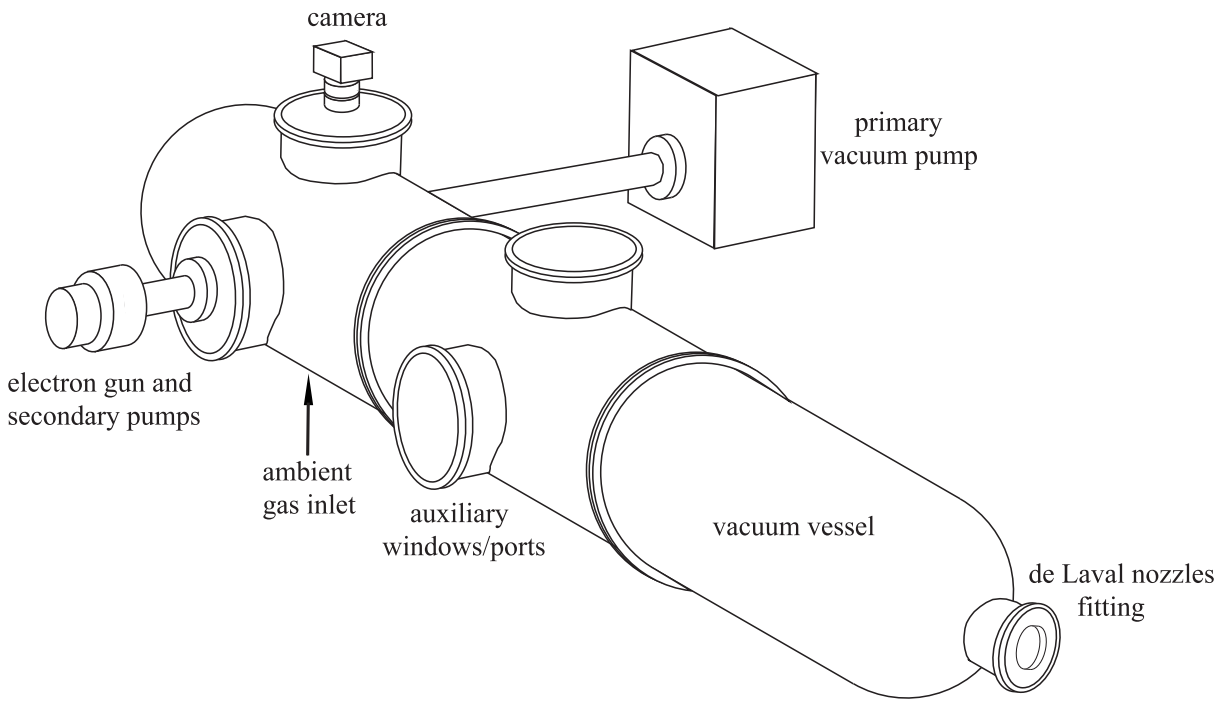

By means of a fast piston, the jet gas is compressed to stagnation pressures in the 0.1 to 0.7 MPa range, and is then accelerated by a de Laval nozzle.

A nozzle designed to generate a $\mathcal{M} = 15$ at the exit has been used in this experiment. Slightly different Mach numbers can be obtained by adjusting the stagnation/ambient pressure ratio p_0/p_a around the value $4.76 \cdot 10^4$.

3 The experiment: facilities

The jet travels along a vessel filled with the desired ambient gas (at pressures in the 1.5 to 100 Pa range) and meets an electron sheet.

The sheet ionizes the gases and makes a plane section of the flow visible, this image is acquired by an intensified CMOS camera.

The vessel is modular and the length is 2.46 m in the present setup. The camera window is 0.27 m wide. The nozzle exit diameter is 0.07136 m.

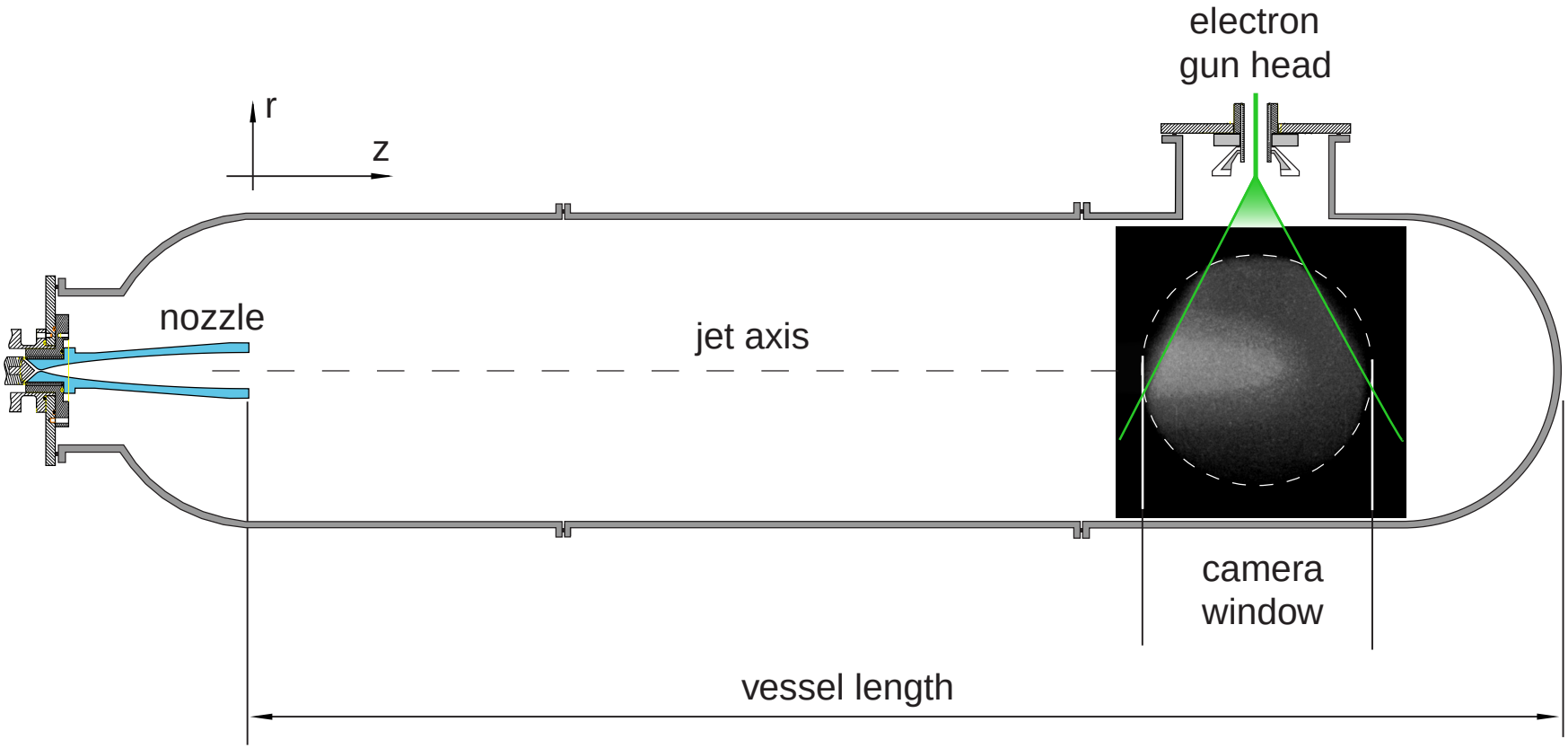

A typical setup for matched jets at M=15

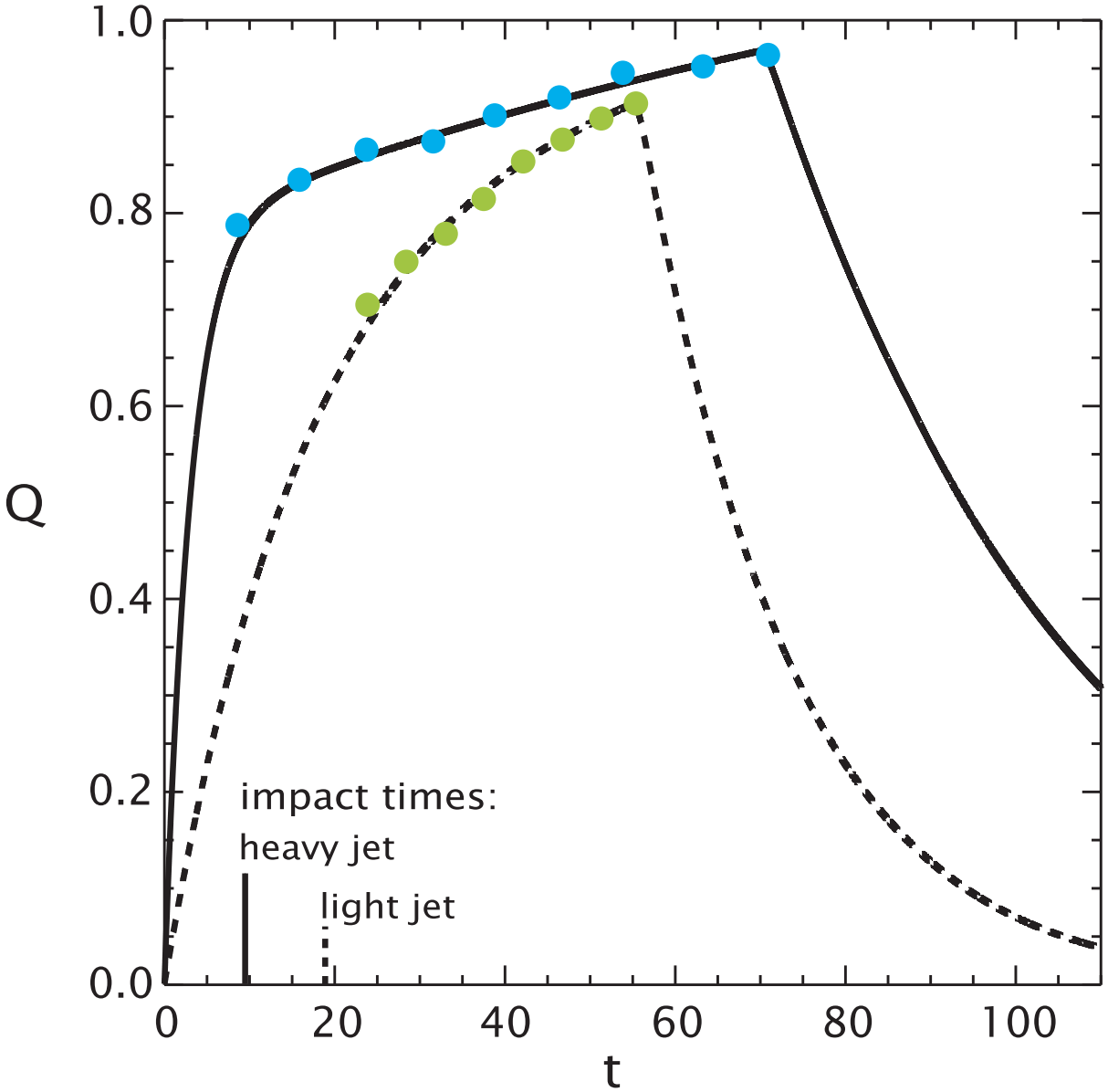
1.0
0.8
0.6
0.4
0.2
0.0
Q
0
20
40
60
80
100
t
impact times:
heavy jet
light jet

Jet gas injection: dimensionless nozzle mass flow versus dimensionless time.

Solid line (numeric) and blue dots (experimental): heavy jet, Xenon in Air. Dashed line (numeric) and green dots (experimental): light jet, Helium in Xenon.

The mass flow Q is normalized over the reference flow rate Q_r which is yielded by the same nozzle when operating in ideal steady conditions.

For the Helium jet, Q_r is 0.43 g/s and for the Xenon jet, Q_r is 2.44 g/s.

Time is normalized over the jet time unit τ (ratio between the jet radius at the nozzle exit and the speed of sound internal to the jet).

The piston output valves begin to open at $t = 0$.

As the piston is working, the outflow increases to a maximum value, then it diminishes as the gas contained in the reservoir is used up.

The mass flow Q is a function of time of the kind

$$Q = Q[p_0(t), f(t), g(t)],$$

where p_0 is the pressure in the piston chamber,
$f(t)$ is a factor function which accounts for the way the nozzle flow is accelerated by the fast piston device, and
$g(t)$ is the function which accounts for the final decay phase due to the emptying of the gas from the piston chamber.
This model, which is based on piston-valve behaviour, gives the following for density, pressure and velocity of the gas at the nozzle exit:

$$\rho_{\rm jet} \sim Q(t)^{2/3},\ p_{\rm jet} \sim Q(t)^{2/3}/\gamma, v_{\rm jet} \sim \mathcal{M}\ Q(t)^{1/3}$$

where $\mathcal{M}$ is the Mach number at the nozzle exit.

During the decreasing phase, the mass flow is determined by the natural decay in the amount of gas remaining in the piston.

4 The numerical code PLUTO, http://plutocode.to.astro.it/

For the solution of hypersonic flows in 1, 2, and 3 spatial dimensions and different systems of coordinates.

The code provides a multiphysics, multialgorithm modular environment particularly oriented toward the treatment of astrophysical flows in presence of discontinuities. Different hydrodynamic modules and algorithms may be independently selected to properly describe Newtonian, relativistic, MHD, or relativistic MHD fluids.

The modular structure exploits a general framework for integrating a system of conservation laws, built on modern Godunov-type shock-capturing schemes. The discretization recipe involves three general steps: a piecewise polynomial reconstruction followed by the solution of Riemann problems at zone interfaces and a final evolution stage.

Comparisons with numerical simulations: An underdense (light) jet, Mach 15, density ratio 0.7

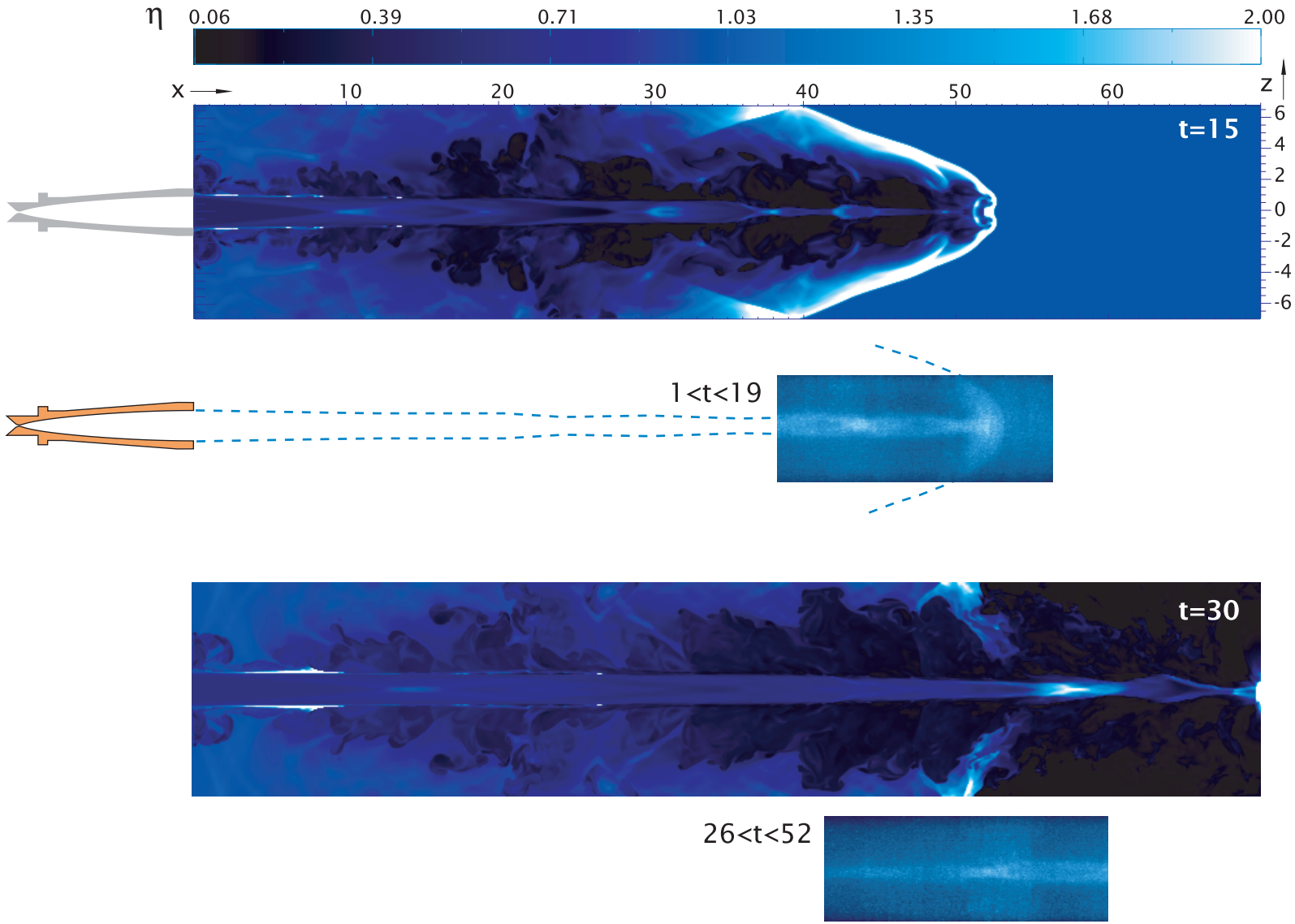

Light jet, Helium in Xenon.

$\mathcal{M}$=16.1, ambient pressure $p_a = 4.0 \pm 0.1$Pa, estimated nozzle exit velocity = 3200 ±330 m/s, mean jet pressure at nozzle exit $p_j = p_a \pm 30\%$, stagnation/ambient pressure ratio $p_0/p_a = 7 \cdot 10^4 \pm 30\%$. Comparison of numerical simulations (density maps) and visualizations (superpositions of scaled correlated frames).

The density maps are normalized to the unperturbed ambient value. The space unit is the exit radius of the nozzle $r_0 = 0.03568$ m. The time unit for this light jet is $\tau = 0.18$ ms.

light jet Movies

LIGHT JET

The interaction with the reflected flow does not spoil the axial-symmetry of the flow. This interaction thus represents a small perturbation. The impact of this jet on the chamber end wall reflects only a very small amount of matter, hence the weak perturbation.

It is also noticeable that the inner part of the flow remains compact and collimated after the impact.

This is also interesting information, which could open the way to other applications, in particular to perturbative near-linear experimental studies.

The inertial effects, and the associated compressibility, must here be exceedingly powerful to inhibit the spatial growth of the jet, unlike what happens in the incompressible situation, where sheared flows spatially thicken.

An overdense (heavy) jet, Mach 15, density ratio 100

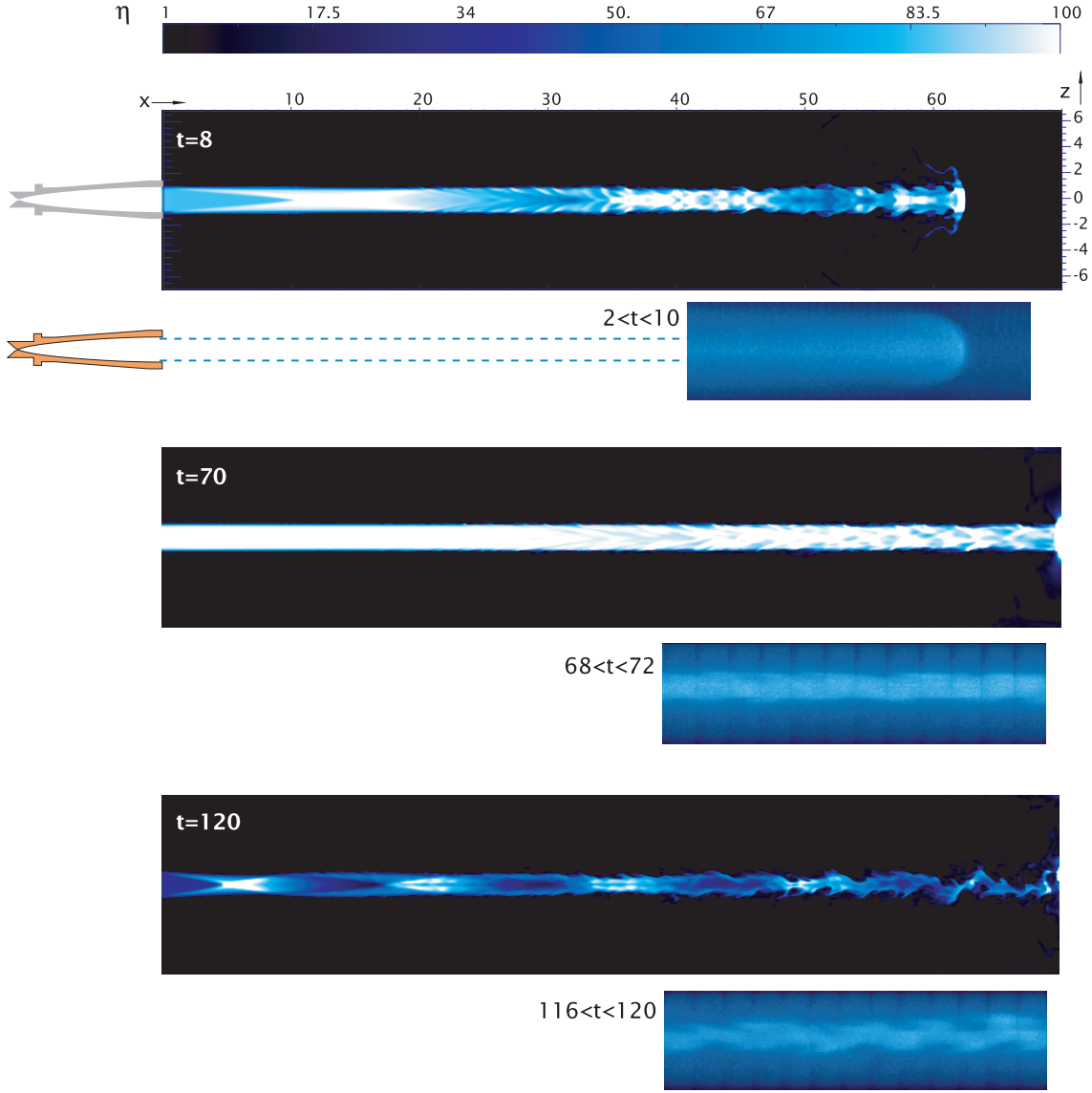

Heavy jet, Xenon in Air.

$\mathcal{M}$=15, ambient pressure $p_a = 9.95 \pm 0.1$ Pa, estimated nozzle velocity at the exit = 560 ± 60m/s, mean jet pressure at the nozzle exit $p_j = p_a \pm 30\%$, stagnation/ambient pressure ratio $p_0/p_a = 4.76 \cdot 10^4 \pm 30\%$. Comparison of numerical simulations (density maps) and visualizations (superpositions of scaled correlated frames).

The density maps are normalized to the unperturbed ambient value. The space unit is the exit radius of the nozzle $r_0 = 0.03568$ m. The time unit for this heavy jet is $\tau = 0.96$ ms.

heavy jet Movies

HEAVY JET

The interaction with the reflected flow eventually produces a finite perturbation, which non linearly interacts with the outflow. This is sufficient to spoil the axial symmetry.

However, it is not sufficient to spoil the collimation of the jet. This suggests the possibility of a very large longitudinal extent of the heavy hypersonic jet and its related capability to transfer energy, momentum and mass to large distances (on the Earth, in space, in possible new applications).

First image reconstructions by correlated frames superposition: a light and a heavy jet at the same Mach number

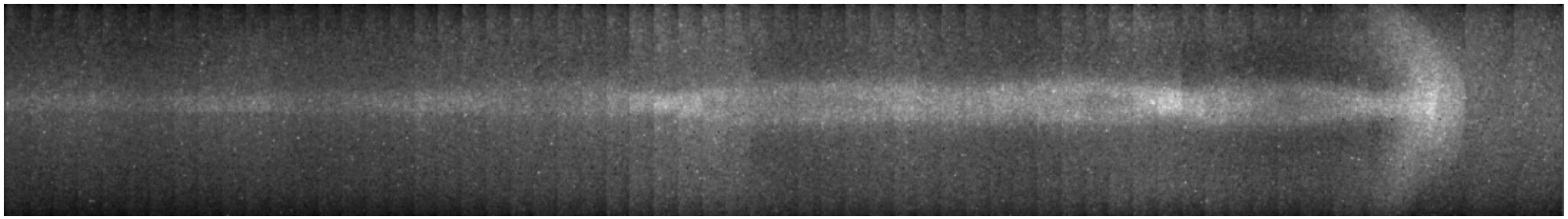

Figure 1: A light jet, He in Xe, $0 < t < 66t_{jet}$

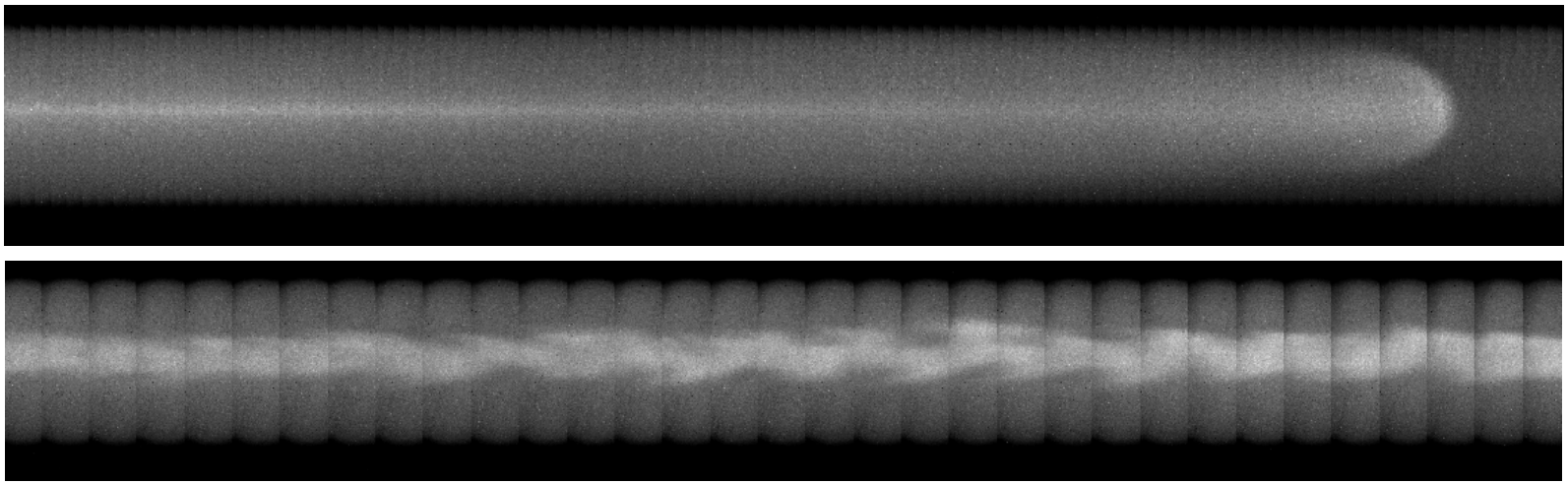

Figure 2: A heavy jet, Xe in Ar, $0 < t < 20t_{jet}$ and $60 < t < 70t_{jet}$

A comparison with an existing experiment (Foster et al. 2005):

At given $\rho_{\rm jet}/\rho_{\rm amb}$, present system permits longer scales and highest Mach numbers

Figure 3: Top: present experiment, $\rho_{\rm jet}/\rho_{\rm amb} \sim 0.7$, $M \sim 15$. Bottom: Foster 2005, $\rho_{\rm jet}/\rho_{\rm amb} \sim 1$, $M \sim 3$

In conclusion:

our experiment highlights the following aspects that are common to astrophysical (stellar) jets:

I) - the high collimation degree of the jets,

II) - the axis symmetry of the jet and its surrounding sheath, and in particular of the portion following the jet head.

These are therefore also properties of high Mach number Newtonian jets, and do not necessitate the confining effects of the magnetic field.

The search for a physical minimum common denominator plays a crucial role in the identification of the elements that are retained in YSO jets.

The point at issue here is that a number of aspects that are specific of the morphology of these jets have appeared in hypersonic jets produced in an Earth laboratory and numerical experiments where only nonlinear Newtonian compressible fluid dynamics applies.

5 Details

Details of the experiment setup

Image correlation techniques and velocity measurements

Details of the numerical method

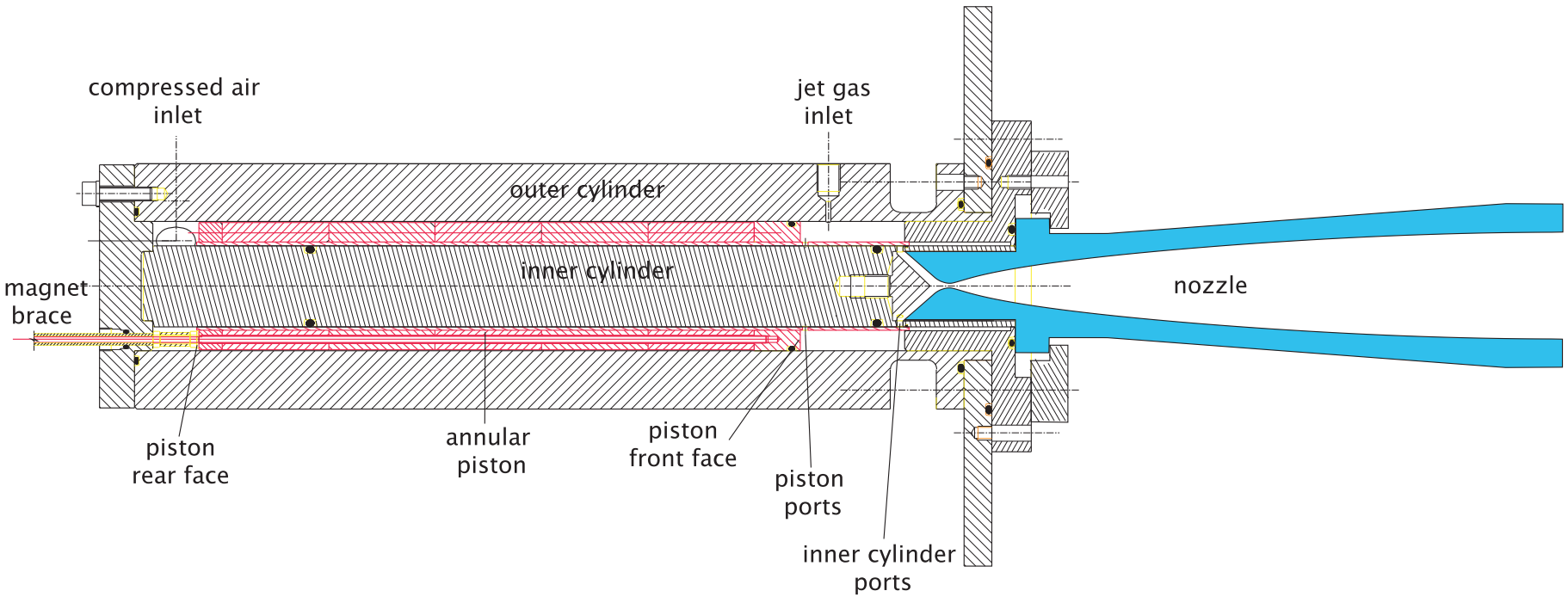

Longitudinal section of the piston-nozzle system. The piston is shown at the starting position.

Piston working

The image correlation technique

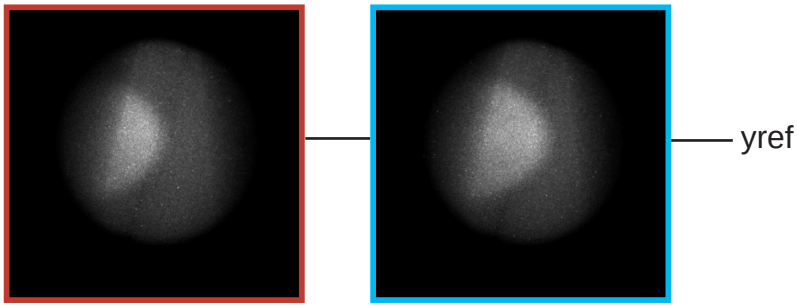

2 consecutive images,
or pixel matrices A_{ij} and B_{ij},
512x512

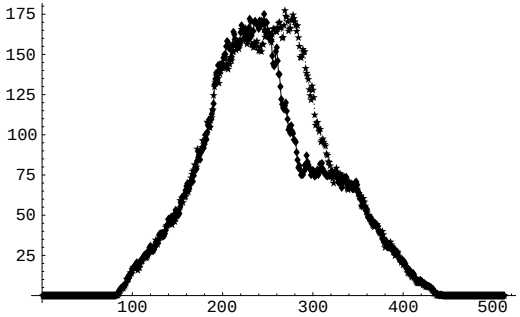

Images intensities (pixel values)
of the 2 images at yref row:
vectors $a_j=A_{nj}$ and $b_j=B_{nj}$ (n=const.)

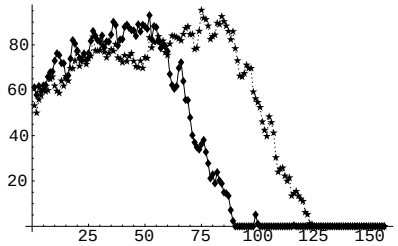

(Intensity - offset), i.e.
curves $a'_j = a_j-c$, $b'_j = b_j-c$,
with c=const.

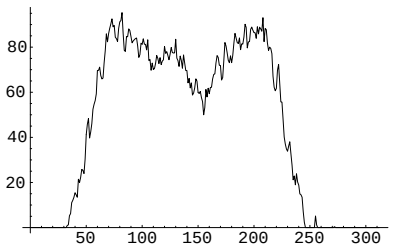

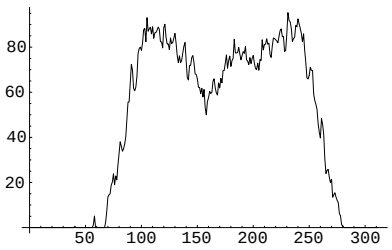

Cross-reflections of the previous curves against results ambiguity:
curves $f_j = a'_j \cup R(b'_j)$, $g_j = b'_j \cup R(a'_j)$
(R: reflection operator)

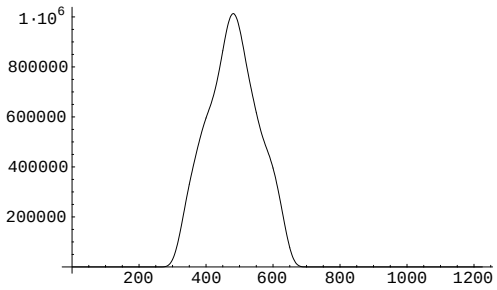

Correlation between the previous curves, i.e.
$h_k = \Sigma_j f_j g_{(j-k)}$.
The abscissa of the maximum h gives
the displacement s between original images
(here s=512-482=30 pixels).
The velocity is v=s/t, where t=interframe time

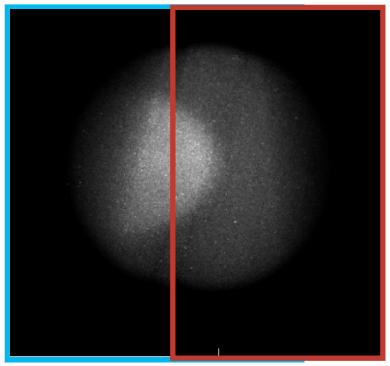

Correlated superposition of the original images

Numerical details

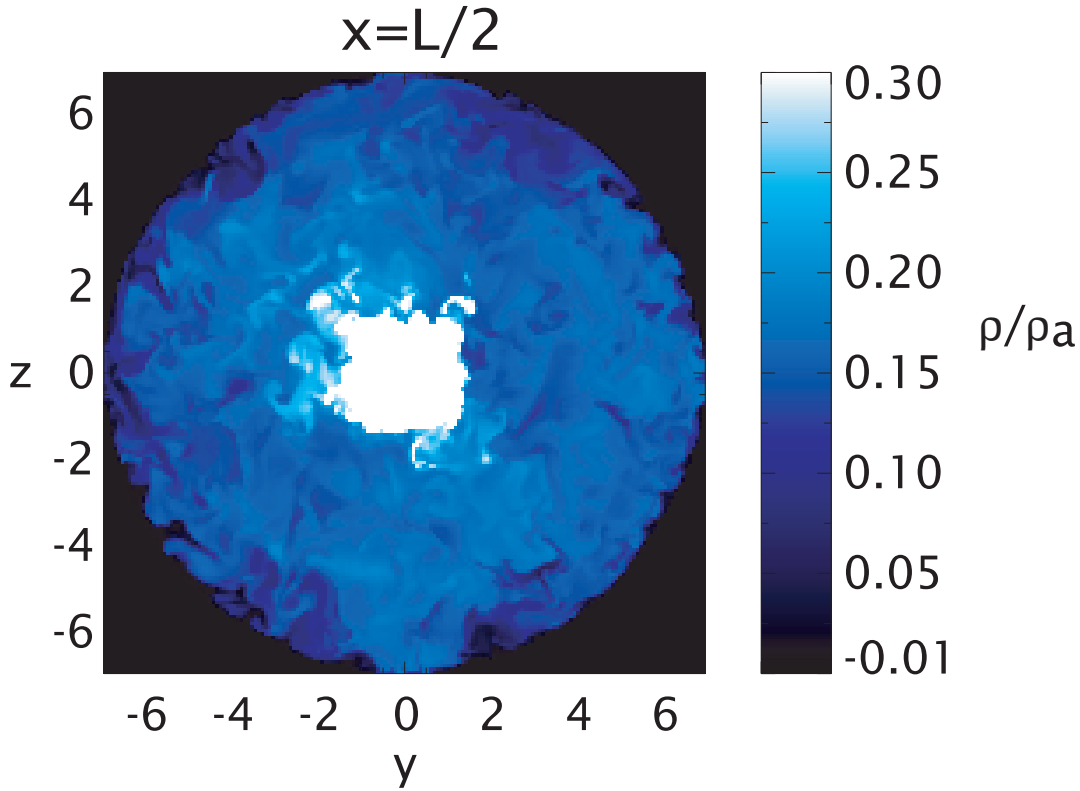

Image of the logarithmic density distribution of the heavy jet for a transverse 2D cut taken at the center of the longitudinal axis and at the time $t = 90$.

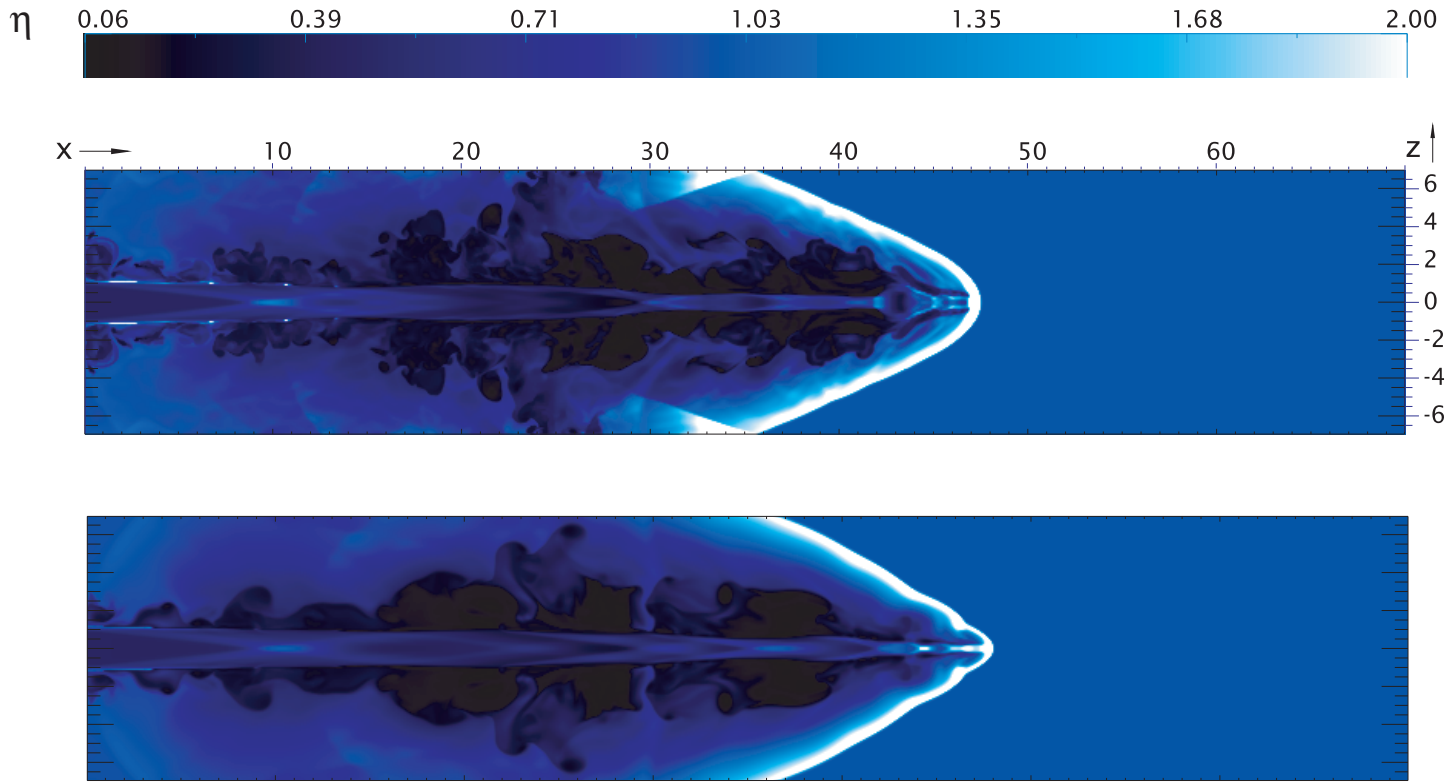

Comparison between simulations with and without lateral boundaries at $t = 14$

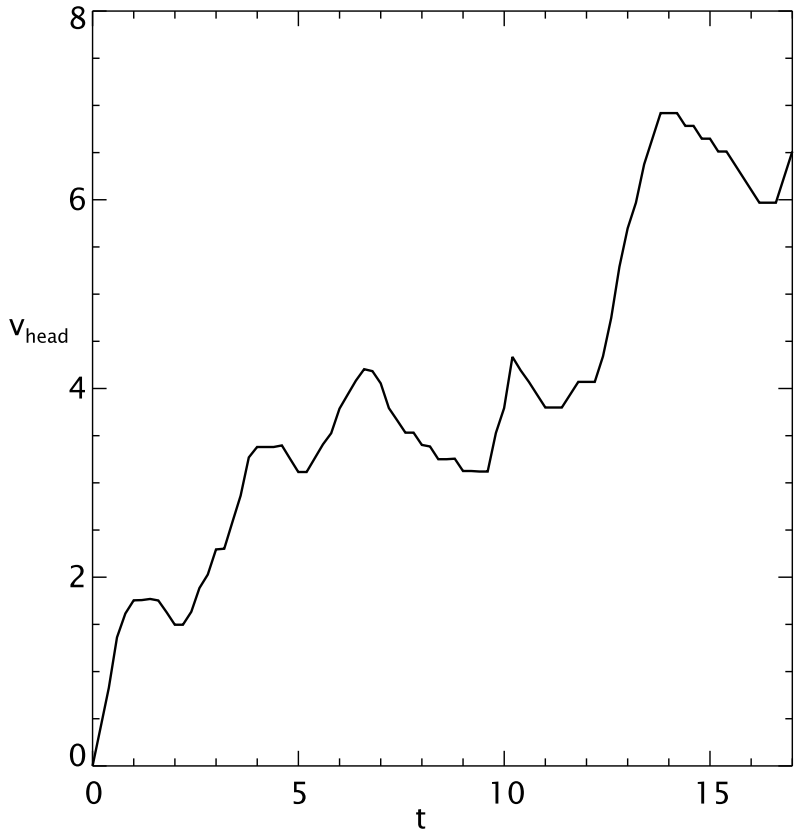

Jet's head velocity in dimensionless r_0/τ units vs dimensionless time for the light jet case and outflow lateral conditions

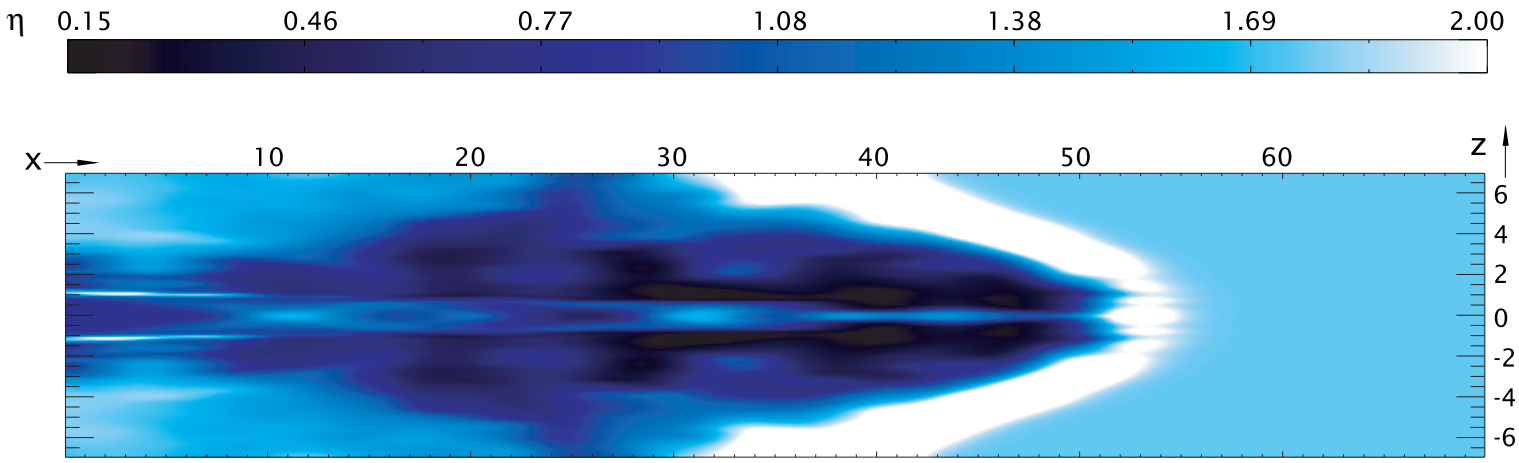

Longitudinal 2D cut at $t = 15$ of the light jet simulation, processed by a longitudinal gaussian convolution to simulate the integrated light acquired by the camera on the exposure time. The gaussian half-widht is 0.25 jet radii

6 Flows under test and physical conditions

	Jet	
	Underexpanded	**Nearly Matched**
Nozzle geometry	**Truncated**	**De Laval**
Stagnation/ambient pressure ratio p_0/p_{amb}	**10 to** 10^5	**300 to** $2 \cdot 10^5$
Mach number M_{max}	**5 to more than 50**	**5 to 20**
Density ratio $\rho_{\mathrm{jet}}/\rho_{\mathrm{amb}}$	**0.04 to 12**	**0.01 to 110**
Reynolds, throat diameter based Re_n	10^3 **to** $5 \cdot 10^4$	10^4 **to** $5 \cdot 10^4$
Reynolds, jet diameter based Re_D	**up to** $5 \cdot 10^5$	**up to** $7 \cdot 10^5$
Reynolds, axial length based Re_x	$> 10^5$	$> 10^6$

7 Fundamentals of measurement techniques

Fluorescent emission of rarefied gases:
Radiant intensity I vs numerical density n (Grün, 1954):

$$I = \frac{k_1\, n}{1 + k_2(T)\, n}$$

Typical fluorescent emission at constant T:

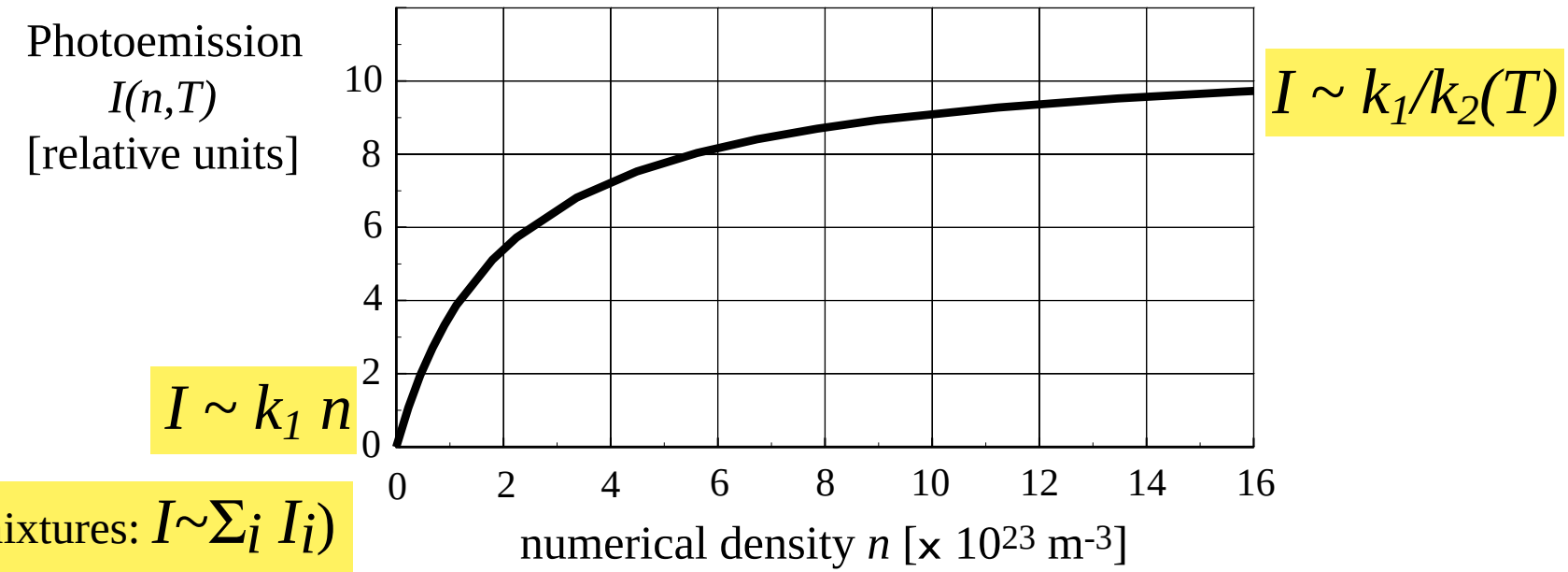

Interchangeable de Laval nozzles

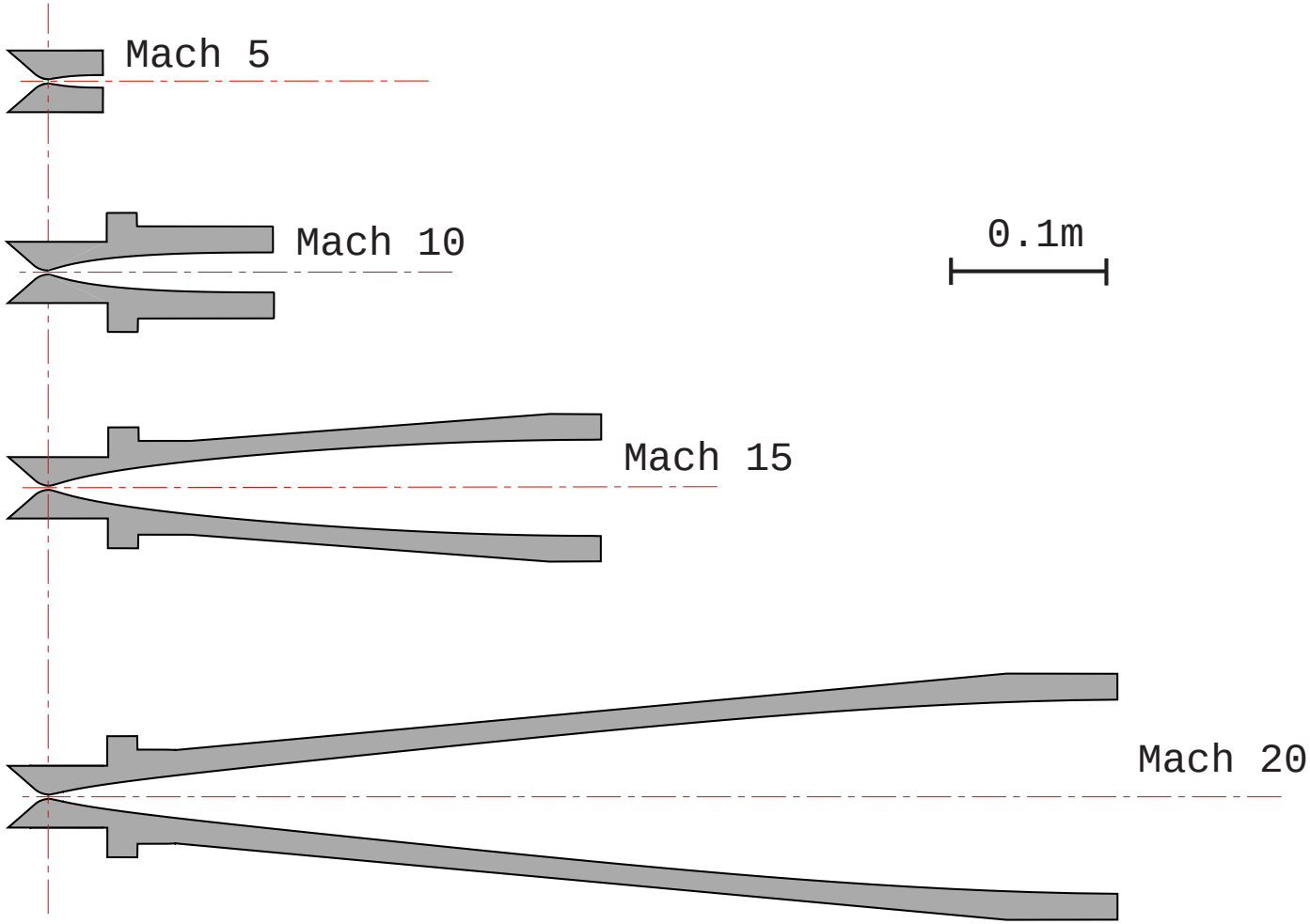

8 References

Belan M., De Ponte S., Tordella D., Highly under-expanded jets in the presence of a transversal density gradient. *in preparation.*

Tordella D., Belan M., Massaglia S., De Ponte S., Mignone A., Ferrari A., Bodenschatz E., Astrophysical jets: insight into long term hydrodynamics. *in preparation.*

Belan M., De Ponte S., Tordella D., Determination of density and concentration from fluorescent images of a gas flow. *Exp Fluids 2008 - vol.45 n3, sept. 2008*

Belan M., De Ponte S., Tordella D., Simultaneous density and concentration measurements on hypersonic jets. *EFMC6 KTH, Euromech Fluid Mechanics Conference 6*, **Royal Institute of technology, Stockholm, 2006.**

Belan M., De Ponte S., Massaglia S., Tordella D., Experiments and numerical simulations on the mid-term evolution of hypersonic jets. *Astrophysics and Space Science 293 (1-2): 225-232*, **2004**

Belan M., De Ponte S., Tordella D., Cross density variations and vorticity generation in compressible shears. *57th APS-DFD, Annual Meeting of the American Physical Society, Division of Fluid Dynamics*, **2004, Seattle, Washington, University of Washington**

Belan M., Tordella D., De Ponte S., A system of fast acceleration of a mass of gas for the laboratory simulation of stellar jets. *ICIASF meeting*, **Cleveland 2001, 409-416**

Belan M., De Ponte S., D'Ambrosio D., Tordella D., Design of an experiment on the spatial evolution of hypersonic jets. *XVI Conferenza AIDAA*, **Palermo, 2001**

extra:
Overdense jets reconstruction

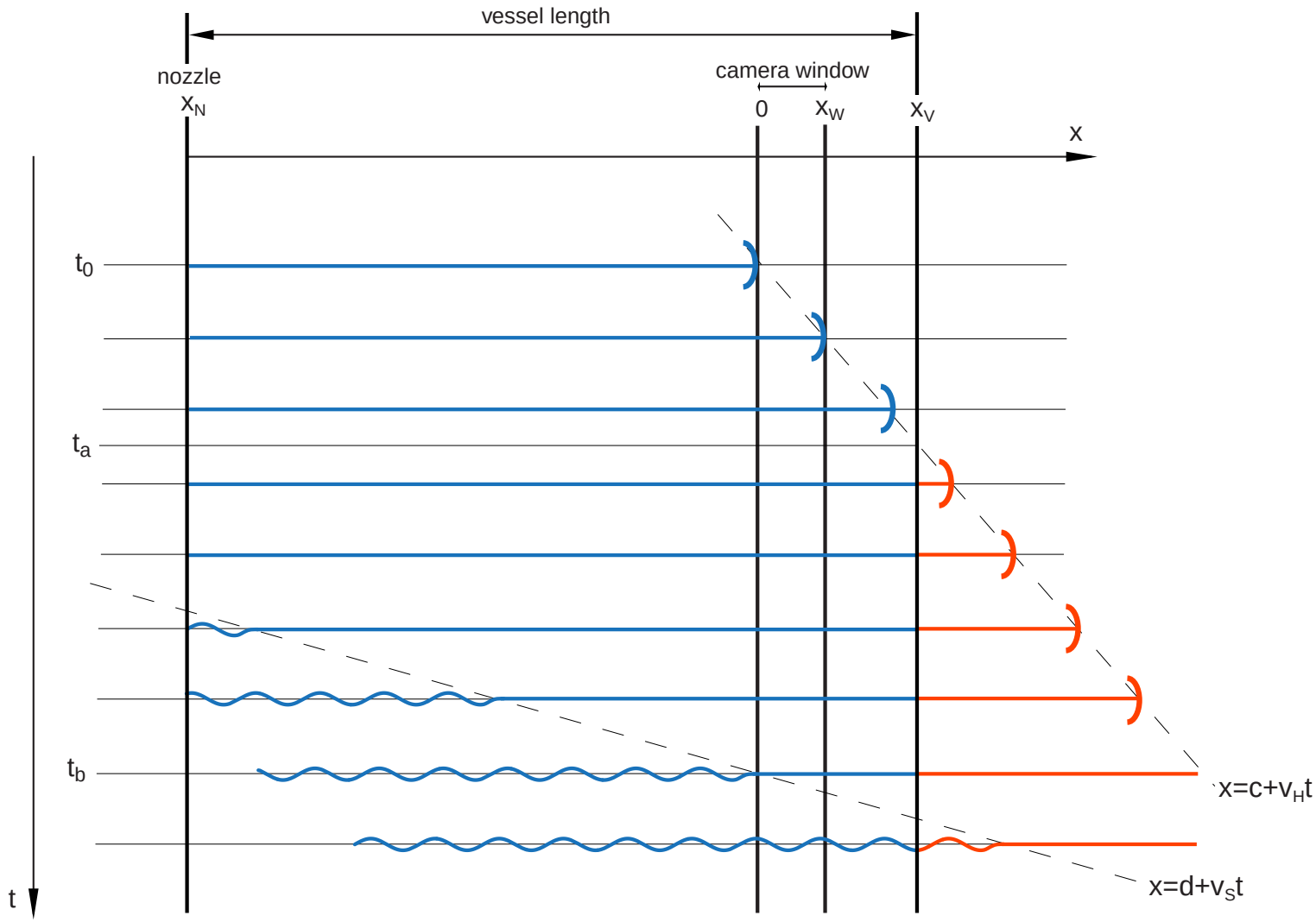

extra:
Underdense jets reconstruction